

# Na Promoted Ni/ $\gamma$ -Al<sub>2</sub>O<sub>3</sub> Catalysts Prepared by Solution Combustion Method for Syngas Methanation

Yan Zeng, Hongfang Ma, Haitao Zhang, Weiyong Ying

**Abstract**—Ni-based catalysts with different amounts of Na as promoter from 2 to 6 wt % were prepared by solution combustion method. The catalytic activity was investigated in syngas methanation reaction. Carbon oxides conversion and methane selectivity are greatly influenced by sodium loading. Adding 2 wt% Na remarkably improves catalytic activity and long-term stability, attributed to its smaller mean NiO particle size, better distribution, and milder metal-support interaction. However, excess addition of Na results in deactivation distinctly due to the blockage of active sites.

**Keywords**—Nickel catalysts, Syngas methanation, Sodium, Solution combustion method.

## I. INTRODUCTION

NATURAL gas is an efficient and clean energy carrier for its high calorific value and complete combustion [1]. Because of its limitation and rising price of oil, coal to synthetic natural gas (SNG) has obtained much attention in recent years among the different way of coal utilization [2]. Although various chemical processes for the production of SNG have been investigated, coal to SNG is known to be one of the major processes for producing SNG [3], [4].

In the coal to SNG process, methane production through syngas methanation has been recognized as a key process [5], [6]. Therefore, developing an efficient catalyst for the methanation reaction would be significant. Since Sabatier and Senderens discovered that some metals (Ni, Rh, Fe and Co) could catalyze the methanation reaction in 1902 [7], many methanation catalysts have been developed. However, Ni-based catalysts are still the most favorable choice for SNG production for its relatively high activity and low price [8], [9]. The requirements to be met by a suitable methanation catalyst are: (1) High activity at a low temperature of approximate 300°C; (2) Sufficient stability at temperature of 500°C or even higher. It is known that nickel/alumina catalysts prepared by conventional methods (coprecipitation, impregnation, sol-gel and mechanical mixing) suffer from severe catalyst deactivation during the methanation reaction due to sintering.

Interestingly, Zhao et al. successfully employed solution combustion method (SCM) to prepare Ni-based catalysts for syngas methanation [10]. The results indicated that Ni-based catalysts prepared by SCM retain high catalytic activity at low-temperature (~300°C) and high stability at high-temperature

(~600°C). SCM is a rapid and simple process for preparing porous materials generally used as catalysts. However successful application of SCM in Ni-based catalysts for syngas methanation, little attention has been paid to the effect of promoters on the catalytic activity. The effect of sodium on the methanation activity of nickel/alumina coprecipitated catalysts had been investigated previously [11], and Huang' group found that alkali is beneficial for carbon monoxide methanation [12]. Herein, we incorporate sodium in Ni-based catalyst prepared by SCM for syngas methanation, and study the impact of Na loading on catalyst activity and stability for syngas methanation. Properties of series Ni-based catalysts modified by different amount of Na were characterized by BET, XRD, TPR, and TEM.

## II. EXPERIMENTAL

### A. Catalyst Preparation

Certain amounts of Ni(NO<sub>3</sub>)<sub>2</sub>·6H<sub>2</sub>O, Na<sub>2</sub>CO<sub>3</sub> and Al(NO<sub>3</sub>)<sub>3</sub>·9H<sub>2</sub>O were dissolved in 200 mL water-glycol (v/v=1:1) under vigorous stirring and then kept at 70°C for 6 h. The mixture placed in an open china crucible was heated to 700°C under static air in a muffle furnace with given heating rate (combustion occurred spontaneously during the heating process), and then kept at 700°C for 7 h. The nickel loading was fixed at 30 wt % while Na loading was varied from 2 to 6 wt%, resulting in catalytic systems called G-2Na, G-4Na, and G-6Na, respectively. The letter 'G' represents the water-glycol solvent, and the letter 'x' stands for the weight percent of Na. For comparison, sodium-free catalyst with 30 wt% Ni loading was prepared by impregnation method and called G-0Na.

### B. Catalyst Characterization

Nitrogen adsorption-desorption isotherms were obtained with a Micrometrics ASAP 2020 apparatus. Prior to N<sub>2</sub> adsorption, the samples were degassed under vacuum at 200°C for 4 h. Specific surface areas were measured by Brunauer Emmet Teller (BET) method. Total pore volume and pore sizes were evaluated using the standard Barrett-Joyner-Halenda (BJH) treatment.

Powder x-ray diffraction (XRD) patterns were recorded on a Rigaku D/Max 2550 using Cu K $\alpha$  radiation at 40 kV and 100 mA. XRD patterns were obtained over a 2 $\theta$  range of 10-80° and a step size of 0.02°.

Hydrogen temperature-programmed reduction (H<sub>2</sub>-TPR) measurements were carried out on Micrometrics AutoChem II 2920. Prior to the H<sub>2</sub>-TPR measurements, 0.0200 g sample placed in a quartz U-tube reactor was pretreated in Ar stream at 500°C for 1.0 h and then cooled to 50°C. H<sub>2</sub>-TPR was

Y.Zeng, W.Y. Ying, H. T. Zhang, and H. F. Ma are with Engineering Research Center of Large Scale Reactor Engineering and Technology, Ministry of Education, State Key Laboratory of Chemical Engineering, the East China University of Science and Technology, Shanghai, 200237 CN (e-mail: zengyan111999@sina.com, wyying@ecust.edu.cn, zht@ecust.edu.cn, mark@ecust.edu.cn, respectively).

conducted with a gas mixture of 10 vol. % H<sub>2</sub> in Ar at a flow rate of 50 mL·min<sup>-1</sup>. Temperature was raised to 1000°C with a heating rate of 10°C·min<sup>-1</sup>. Hydrogen consumption was measured by a thermal conductivity detector (TCD).

Transmission electron microscope (TEM) images were taken by means of a JEM-1400 apparatus operating at 100KV. In order to obtain suitable samples, the catalyst powders were dispersed in ethanol by ultrasonic and then a drop of the solution was placed on a carbon-coated copper grid.

### C. Syngas Methanation

Syngas (carbon oxides and hydrogen) methanation reactions were carried out in a 12 mm (inner diameter) fixed-bed reactor. The reactions were performed at 0.1 MPa, temperature range of 300-400°C, while high temperature stability tests were carried out at 600°C, 2 MPa, and with 30 mol. % of water. Typically, 0.5000 g catalyst was used, and the total gas flow rate was 93 mL·min<sup>-1</sup>, corresponding to a weight hourly space velocity (WHSV) of 12000 mL·g<sup>-1</sup>·h<sup>-1</sup>. The catalyst diluted with certain amount of inert Al<sub>2</sub>O<sub>3</sub> was settled in the uniform temperature zone, where the axial temperature was measured with a thermocouple through the catalyst bed. Prior to the reaction, the catalyst was heated from ambient to 700°C with a heating rate of 2°C·min<sup>-1</sup> and reduced for 3 h in situ by pure hydrogen. The catalyst was then cooled to 300°C under nitrogen flow and the reaction started as gas flow was switched to the syngas (15.4 vol. % CO, 10.3 vol. % CO<sub>2</sub>, 69.2 vol. % H<sub>2</sub>, and 5.1 vol. % N<sub>2</sub>). Flow rates of all gases were monitored by calibrated mass flow controllers (Brooks 5850 E).

Gas compositions of the inlet and outlet were analyzed by an on-line gas chromatography (Agilent 7890A series) equipped with one FID (flame ionization detector) and two TCD (thermal conductivity detector). Hydrocarbons from C<sub>1</sub> to C<sub>6</sub> were analyzed by a FID after separation with a HP-PLOT "S" Al<sub>2</sub>O<sub>3</sub> column. N<sub>2</sub>, CO and CO<sub>2</sub> were analyzed by a TCD after separation with two PropackQ and one 5Å molecular sieve columns (CO<sub>2</sub> did not enter this column). H<sub>2</sub> was analyzed using a TCD after separation with one PropackQ and one 5Å molecular sieve column. To calculate carbon oxides conversion, formation rate and selectivity of methane, the effluent gas were analyzed after steady-state operation under each condition. Here, we define:

CO conversion:

$$X_{\text{CO}}(\%) = \frac{N_{\text{CO},\text{in}} - N_{\text{CO},\text{out}}}{N_{\text{CO},\text{in}}} \times 100 \quad (1)$$

CO<sub>2</sub> conversion:

$$X_{\text{CO}_2}(\%) = \frac{N_{\text{CO}_2,\text{in}} - N_{\text{CO}_2,\text{out}}}{N_{\text{CO}_2,\text{in}}} \times 100 \quad (2)$$

CH<sub>4</sub> selectivity:

$$S_{\text{CH}_4}(\%) = \frac{N_{\text{CH}_4,\text{out}}}{(N_{\text{CO},\text{in}} - N_{\text{CO},\text{out}}) + (N_{\text{CO}_2,\text{in}} - N_{\text{CO}_2,\text{out}})} \times 100 \quad (3)$$

CH<sub>4</sub> formation rate:

$$r_{\text{CH}_4} = \frac{N_{\text{CH}_4,\text{out}}}{m_{\text{Ni}}} \quad (4)$$

N is the mole flow rate (mol·h<sup>-1</sup>), and m is the weight of Ni (g).

## III. RESULTS AND DISCUSSION

The N<sub>2</sub> adsorption-desorption isotherms and the pore size distributions of as-synthesized Ni-Al<sub>2</sub>O<sub>3</sub> catalysts are shown in Fig. 1. All the isotherms present a typical type IV curve, which was characteristic of mesoporous material. Compared with Na modified catalysts, G-0Na retains two peaks of pore size distribution that indicates the introduction of Na was beneficial for the uniform pore size.

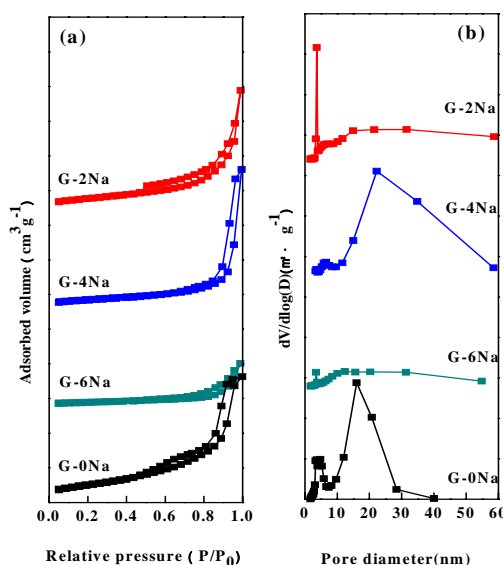


Fig. 1 (a) N<sub>2</sub> adsorption-desorption isotherms, and (b) pore size distributions

The textural properties of the four catalysts are listed in Table I. The surface area, pore volume and average pore diameter of the G-6Na is lower than that of the other catalysts. It may be the blockage of parts of small pores caused by Na loading.

TABLE I  
SURFACE AREA, PORE VOLUME, AVERAGE PORE DIAMETER AND NiO CRYSTAL SIZE FOR FRESH CALCINED Ni-Al<sub>2</sub>O<sub>3</sub> CATALYSTS, AND Ni CRYSTAL SIZE FOR REDUCED Ni-Al<sub>2</sub>O<sub>3</sub> CATALYSTS

Sample	S <sub>BET</sub> (m <sup>2</sup> ·g <sup>-1</sup> )	V <sub>p</sub> <sup>a</sup> (cm <sup>3</sup> ·g <sup>-1</sup> )	D <sub>p</sub> <sup>b</sup> (nm)	D <sub>NiO</sub> <sup>c</sup> (nm)	D <sub>Ni</sub> <sup>c</sup> (nm)
G-2Na	67.1	0.271	12.2	17.7	22.0
G-4Na	46.1	0.310	21.5	18.5	24.5
G-6Na	17.6	0.095	6.3	19.0	25.5
G-0Na	93.5	0.282	13.7	22.7	25.7

<sup>a</sup> BJH desorption pore volume.

<sup>b</sup> BJH desorption average pore diameter.

<sup>c</sup> Calculated from XRD using Scherrer equation

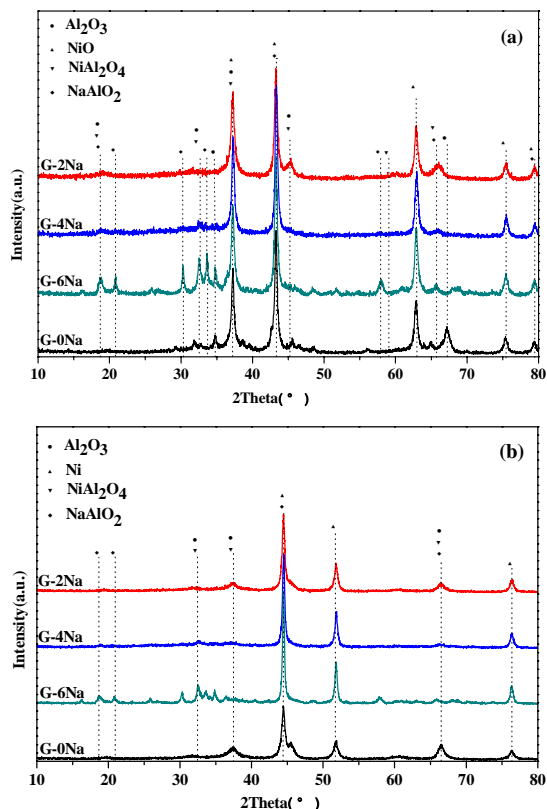


Fig. 2 XRD patterns of fresh calcined Ni-Al<sub>2</sub>O<sub>3</sub> catalysts (a), and reduced catalysts (b), respectively

XRD patterns of fresh calcined as well as reduced Ni-Al<sub>2</sub>O<sub>3</sub> catalysts are shown in Figs. 2 (a) and (b), respectively. For the four fresh calcined catalysts, the diffraction peaks at 37.3°, 45.6° and 65.8° are attributed to  $\gamma$ -Al<sub>2</sub>O<sub>3</sub> (JCPDS 10-0425), the diffraction peaks at 37.0°, 45.2°, 59.7° and 66.6° are attributed to NiAl<sub>2</sub>O<sub>4</sub> (JCPDS 10-0339), and the diffraction peaks at 37.2°, 43.3°, 62.9° and 75.5° derive from NiO (JCPDS 65-6920). No sodium oxide crystalline phase was detected in G-2Na and G-4Na, suggesting that sodium species are finely dispersed on the catalysts surface and thereby result in the formation of small sodium particles that are below the detection limit of XRD measurements [13]. On increasing Na loading further to 6 wt%, weak reflections due to NaAlO<sub>2</sub> were visible, indicating an increase in the number and size of crystalline sodium oxides particles.

For the reduced Ni-Al<sub>2</sub>O<sub>3</sub> catalysts, the diffraction peaks at 44.5°, 51.8° and 76.3° are attributed to distinct peaks of Ni (JCPDS04-0850). As shown in Fig. 2 (b), distinct peaks of NiAl<sub>2</sub>O<sub>4</sub> and NaAlO<sub>2</sub> still exist in catalysts, implying NiAl<sub>2</sub>O<sub>4</sub> and NaAlO<sub>2</sub> is difficult to be reduced under our experiment condition.

The crystallite sizes of NiO and Ni, calculated using the famous Scherrer equation, are listed in Table I. Mean NiO and Ni particle size of Na modified catalysts is smaller than that of G-0Na. It reveals that adding sodium can increase nickel dispersion and obtain smaller Na particles. The dispersion

effect can be seen clearly in TEM images later.

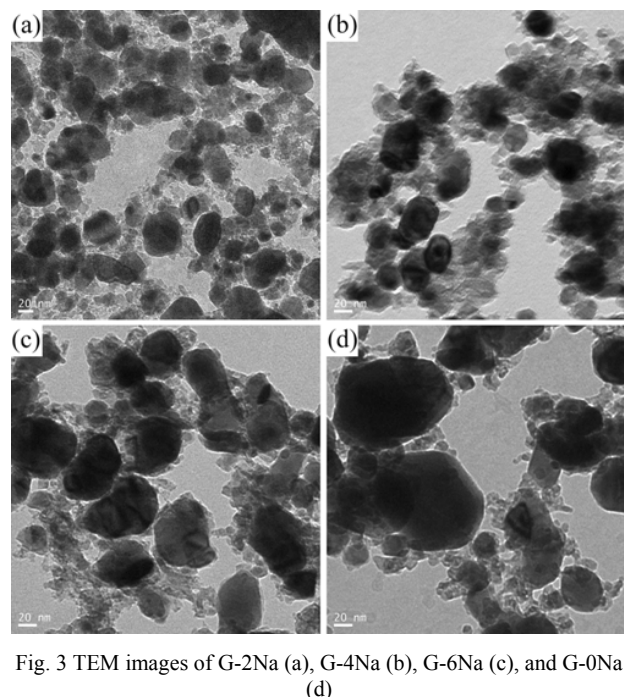


Fig. 3 TEM images of G-2Na (a), G-4Na (b), G-6Na (c), and G-0Na (d)

TEM images of the four reduced samples are shown in Fig. 3. Nickel oxide particles are uniformly dispersed in the cotton-like-Al<sub>2</sub>O<sub>3</sub>. Obviously, nickel dispersions in the sodium modified catalysts are higher than that in G-0Na. The Na doped catalysts have a smaller Ni particle size and narrower distribution of Ni particle. The results are in line with that from XRD. The smaller size means the higher dispersion of metal species, so G-2Na has more active sites in syngas methanation [14], [15], which would be profitable for the catalysis activity.

TPR technique allows us not only to characterize the metal-support interactions but also to elucidate the role of additives as promoters in the reduction process [16]. Several TPR studies on nickel-supported catalysts have been undertaken [13], [17], indicating that Ni<sup>2+</sup> is directly reduced to metallic Ni<sup>0</sup> without any intermediate species, therefore each peak is believed to match a different species. Fig. 4 shows TPR results of the four samples, in which the various peak temperatures reveal the different interaction between nickel oxides and alumina. According to the peaks in their TPR profiles and reported in literatures [16], [18]-[20], the reducible NiO species can be classified into three types:  $\alpha$ ,  $\beta$  and  $\gamma$ . The small peaks located in the low temperature region (300-500 °C) are assigned to  $\alpha$ -type NiO species (surface amorphous NiO or bulk NiO), which are free nickel oxides species and have a weak interaction with alumina. The mild-temperature peaks (500-700°C) represent  $\beta$ -type NiO species (weakly interacted with Al<sub>2</sub>O<sub>3</sub> or called Ni-rich phase), which are the main sources of low-temperature activity after reduction. The high-temperature peaks (>700°C) are assigned to  $\gamma$ -type NiO species (Strongly interact or chemically bound with Al<sub>2</sub>O<sub>3</sub>), which are ascribed to the stable nickel aluminate phase with a

spinel structure.

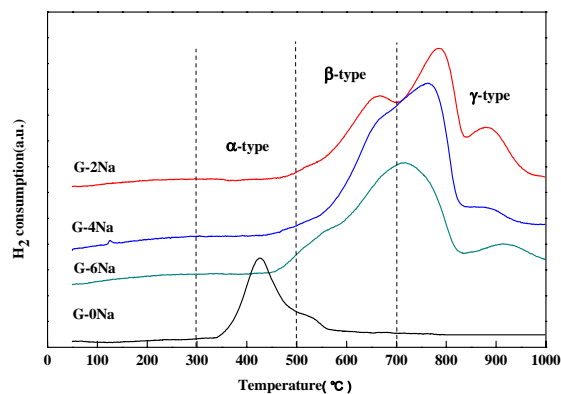


Fig. 4 TPR profiles of the four fresh calcined catalysts

Obviously, in contrast to G-0Na, the reduction peaks of Na modified catalysts shift to higher temperature, implying a relatively stronger metal-support interaction between Ni oxides species and support. The  $\beta$ -type NiO species possessing milder metal-support interaction suggest high catalytic activity and good thermal stability [21]. From TPR profiles, the  $\beta$ -type NiO species in G-2Na is apparently more than that in the other catalysts. These results may hence imply a better catalytic activity of G-2Na for syngas methanation.

Low temperature catalytic activity of the Ni-based catalysts was studied under the condition of  $12000\text{ h}^{-1}$ , 0.1 MPa, and temperatures from 300 to 400°C. CO and CO<sub>2</sub> conversion, and CH<sub>4</sub> selectivity over the four samples are summarized in Fig. 5 (a), (b), and (c), respectively. Higher catalytic activity is observed over G-2Na in comparison with the rest of samples. Moreover, the catalytic activity is closely related to the sodium incorporation amount. When the Na weight percent is 2%, the CO and CO<sub>2</sub> conversion, and CH<sub>4</sub> selectivity reach the highest values. As the sodium amount further increases, the catalytic activity significantly decreases.

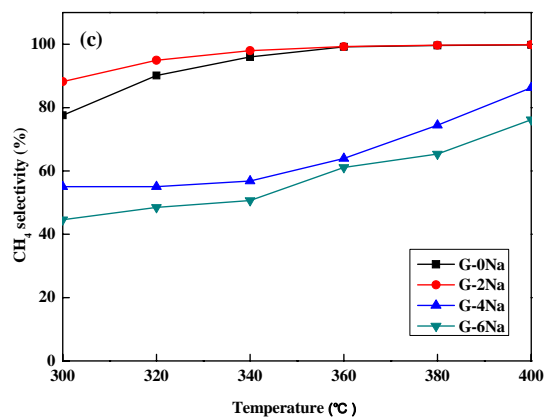
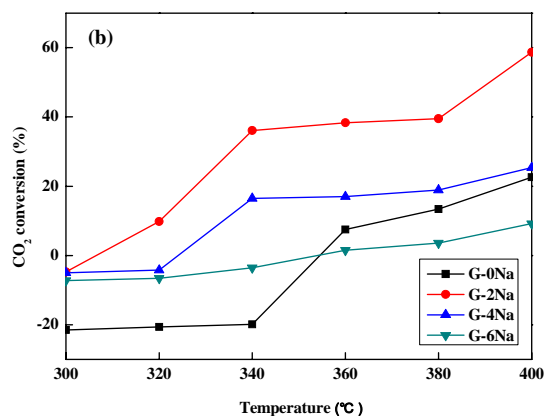
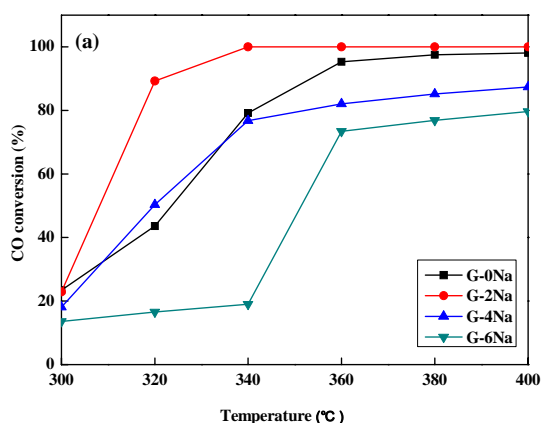


Fig. 5 Effect of Na loading on CO conversion (a), CO<sub>2</sub> conversion (b), and CH<sub>4</sub> selectivity (c)

The high catalytic activity of G-2Na is attributed to the high dispersion Ni nanoparticles and more  $\beta$ -type NiO species (milder meta-support interaction). However, with increasing the doping amount of sodium, catalytic activity decreased distinctly. The loss of activity with higher sodium content is due to the blockage of active sites by excess amounts of sodium introduced to the catalyst, followed by a poisoning via direct metal interaction or support modification by the sodium [12]. Therefore, the optimal sodium loading is 2 wt% concluded from the above facts.

Requirement to be met by a suitable methanation catalyst is the sufficient stability under high temperature. The stability of G-0Na and G-2Na for syngas methanation were investigated on stream for 50 h at 600 °C, 2 MPa,  $120000\text{ mL}\cdot\text{g}^{-1}\cdot\text{h}^{-1}$ , and with 30 mol.% stream. According to Fig. 6, catalyst G-0Na deactivates gradually while G-2Na possesses better high temperature stability. It can be explained by the important characteristics that nickel nanoparticles highly dispersed over the catalyst surface, which result in strong resistance to the carbon deposition and good thermal stability [21]. Therefore, G-2Na with the addition of 2 wt% Na as promoter would be able to ensure long-term stability compared with G-0Na.

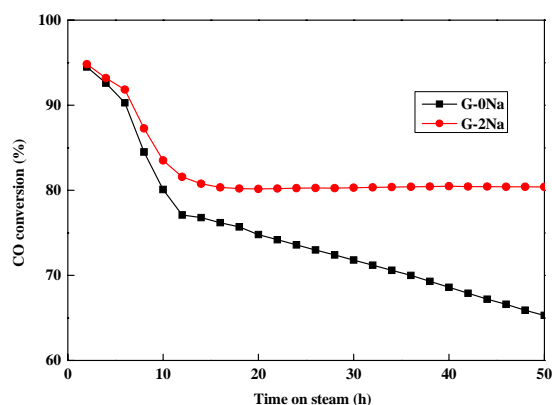


Fig. 6 High temperature stability test over G-0Na and G-2Na at 600 °C, 2 MPa, 120000 mL·g<sup>-1</sup>·h<sup>-1</sup>

#### IV. CONCLUSION

Ni-based catalysts with various Na loading were prepared by solution combustion method, and their properties were characterized in more detail by BET, XRD, TEM, and TPR. Several conclusions can be drawn from these investigations. First, the addition of sodium can change the reduction characteristics of catalysts. G-2Na with 2 wt% Na loading possessed more  $\beta$ -type NiO species (milder metal-support interaction), suggesting high catalytic activity and good thermal stability. Second, doping certain amount of sodium can improve the dispersion of Ni particles, which leads to higher distribution while excessive addition would cause deactivation quickly. Therefore, with 2 wt % Na is optimal in this work. Third, catalyst prepared by SCM with 2 wt % Na loading obtained better high temperature stability than Na-free catalyst in our tests.

#### ACKNOWLEDGMENT

The authors gratefully acknowledge the financial support of the National Science and Technology Supporting Plan of China (2012AA050102).

#### REFERENCES

- [1] S. L. Ma, Y. S. Tan, and Y. Z. Han, "Methanation of syngas over coral reef-like Ni/Al<sub>2</sub>O<sub>3</sub> catalysts", *J. Nat. Gas. Chem.*, vol. 20, pp. 435-440, 2011.
- [2] J. Kopyscinski, T. J. Schildhauer, and S. M. A. Biollaz, "Production of synthetic natural gas (SNG) from coal and dry biomass-A technology review from 1950 to 2009", *Fuel*, vol. 89, pp. 1760-1783, 2010.
- [3] S. Hwang, J. Lee, U. G. Hong, J. G. Seo, J. C. Jung, D. J. Koh, H. Lim, C. Byun, and I. K. Song, "Methane production from carbon monoxide and hydrogen over nickel-alumina xerogel catalyst: Effect of nickel content", *J. Ind. Eng. Chem.*, vol. 17, pp. 154-157, 2011.
- [4] R. W. R. Zwart, and H. Boerrigter, "High Efficiency Co-production of Synthetic Natural Gas (SNG) and Fischer-Tropsch (FT) Transportation Fuels from Biomass", *Energy Fuels*, vol. 19, no. 2, pp. 591-597, 2005.
- [5] P. Panagiotopoulou, D. I. Kondarides, and X. E. Verykios, "Selective methanation of CO over supported noble metal catalysts: Effects of the nature of the metallic phase on catalytic performance", *Appl. Catal. A: Gen.*, vol. 344, no. 1-2, pp. 45-54, 2008.
- [6] Z. Pan, M. Dong, X. Meng, X. Zhang, X. Mu, B. Zong, "Integration of magnetically stabilized bed and amorphous nickel alloy catalyst for CO methanation", *Chem. Eng. Sci.*, vol. 62, no. 10, pp. 2712-2717, 2007.
- [7] P. Sabatier, and J. B. Senderens, "New methane synthesis", *Acad. Sci.*, vol. 134, pp. 514-516, 1902.
- [8] Y. S. Mok, H. C. Kang, H. J. Lee, D. J. Koh, and D. N. Shin, "Effect on nonthermal plasma on the methanation of carbon monoxide over nickel catalyst", *Plasma Chem. Plasma Process.*, vol. 30, pp. 437-447, 2010.
- [9] J. Sehested, S. Dahl, J. Jacobsen, and J. R. Rostrup-Nielsen, "Methanation of CO over nickel: mechanism and kinetics at high H<sub>2</sub>/CO ratios", *J. Phys. Chem. B*, vol. 109, pp. 2432-2438, 2005.
- [10] A. M. Zhao, W. Y. Ying, H. T. Zhang, H. F. Ma, and D. Y. Fang, "Ni-Al<sub>2</sub>O<sub>3</sub> catalysts prepared by solution combustion method for syngas methanation", *Catal. Commun.*, vol. 17, pp. 34-38, 2012.
- [11] E. C. Kruissink, H. L. Pelt, J. R. H. Ross, and L. L. Van Reuen, "The effect of sodium on the methanation activity of nickel/alumina coprecipitated catalysts", *Appl. Catal.*, vol. 1, pp. 23-29, April 1981.
- [12] C. P. Huang, and J. T. Richardson, Alkali promotion of nickel catalysts for carbon monoxide methanation, *J. Catal.* vol. 51, pp. 1-8, 1978.
- [13] C. W. Hu, J. Yao, H. Q. Yang, Y. Chen, and A. M. Tian, "On the Inhomogeneity of Low Nickel Loading Methanation Catalyst", *J. Catal.*, vol. 166, no. 1, pp. 1-7, February 1997.
- [14] N. Wang, K. Shen, L. H. Huang, X. P. Yu, W. Z. Qian, and W. Chu, "Facile route for synthesizing ordered mesoporous Ni-Ce-Al oxide materials and their catalytic performance for methane dry reforming to hydrogen and syngas", *ACS. Catal.*, vol. 3, no. 7, pp. 1638-1651, June 2013.
- [15] J. J. Gao, C. M. Jia, M. J. Zhang, F. N. Gu, G. W. Xu, and F. B. Su, "Effect of nickel nanoparticle size in Ni/ $\alpha$ -Al<sub>2</sub>O<sub>3</sub> on CO methanation reaction for the production of synthetic natural gas", *Catal. Sci. Technol.*, vol. 3, pp. 2009-2015, 2013.
- [16] J. Zhang, H. Y. Xu, X. L. Jin, Q. J. Ge, and W. Z. Li, "Characterizations and activities of the nano-sized Ni/Al<sub>2</sub>O<sub>3</sub> and Ni/La-Al<sub>2</sub>O<sub>3</sub> catalysts for NH<sub>3</sub> decomposition", *Appl. Catal. A: Gen.*, vol. 290, no. 1-2, pp. 87-96, August 2005.
- [17] F. Ocampo, B. Louis, and A. C. Roger, "Methanation of carbon dioxide over nickel-based Ce<sub>0.72</sub>Zr<sub>0.28</sub>O<sub>2</sub> mixed oxide catalysts prepared by sol-gel method", *Appl. Catal. A: Gen.*, vol. 369, no. 1-2, pp. 90-96, November 2009.
- [18] C. Guimon, A. Auroux, E. Romero, and A. Monzon, "Acetylene hydrogenation over Ni-Si-Al mixed oxides prepared by sol-gel technique", *Appl. Catal. A: Gen.*, vol. 251, no. 1, pp. 199-214, 2003.
- [19] Y. H. Zhang, G. X. Xiong, S. S. Sheng, S. L. Liu, and W. S. Yang, "Interaction of NiO with  $\gamma$ -Al<sub>2</sub>O<sub>3</sub> supporter of NiO/ $\gamma$ -Al<sub>2</sub>O<sub>3</sub> catalysts", *Acta. Phys. Chem. Sim. (Wuli Huaxue Xuebao)*, vol. 15, no. 8, pp. 735-741, 1999.
- [20] J. M. Rynkowski, T. Paryczak, and M. Lenik, "On the nature of oxidic nickel phases in NiO/ $\gamma$ -Al<sub>2</sub>O<sub>3</sub> catalysts", *Appl. Catal. A: Gen.*, vol. 106, no. 1, pp. 73-82, 1993.
- [21] D. C. Hu, J. J. Gao, Y. Ping, L. H. Jia, P. Gunawan, Z. Y. Zhong, G. W. Xu, F. N. Gu, and F. B. Su, "Enhanced investigation of CO methanation over Ni/Al<sub>2</sub>O<sub>3</sub> catalysts for synthetic natural gas production", *Ind. Eng. Chem. Res.*, vol. 51, pp. 4875-4886, 2012.